DOI: 10.31401/WS.2025.proc.07

Two Interacting CMEs and Related Eruptions

Koleva K., Duchlev P.

Space Research and Technology Institute, Bulgarian Academy of Sciences
kkoleva@space.bas.bg

Abstract

We investigate the morphology and kinematic characteristics of prominence eruption, occurring in the east solar limb on 2010 June 20. The event was observed by the Atmospheric Imaging Assembly (AIA) on board the Solar Dynamics Observatory (SDO) and by the STEREO Observatory. Two successive CMEs were linked to the eruption. We examine the associated CMEs' kinematics. The observed eruptions showed a strong non-radial motions towards the equator. We study the non radial latitudinal offset of the prominence eruption and related CMEs.

Keywords: solar eruptions; coronal mass ejection; non-radial motion

1. Introduction

One of the most studied phenomena in the solar atmosphere is solar prominences, which are also called filaments when viewed against the solar disk. They are dense and cool structures that stretch outward into the hot and thin solar corona [Tandberg-Hanssen, 1995; Mackay et al.; 2010, Parenti, 2014]. The prominences may become unstable and erupt under certain conditions. It is known that prominence eruptions are part of a larger single eruption that can result in producing a coronal mass ejection (CME) and a solar flare [Forbes, 2000; Priest & Forbes, 2002]. White-light coronagraph images show the erupted prominence material as a bright core of the CME structure.

There are typically two stages to the filament/prominence eruption's kinematic evolution: a slow-rise phase, during which the filament gradually rises with very low acceleration, followed by a sudden transition to a fast-acceleration phase [Sterling et al., 2007].

Observations show that during their eruption, prominences and CMEs can occasionally deviate from the radial direction [Gopalswamy & Thompson, 2000; Koleva et al., 2024]. According to observations CMEs can deflect by ten or more degrees from the source location. Both the prominences and the CMEs show non-radial motions, and therefore, the CME deflects as a whole.

The propagation of CMEs is one of the primary factors affecting space weather on Earth. Changing the propagation's direction can seriously affect the CME's arrival time at 1 AU. Therefore, accurate space weather forecasting requires an understanding of the life cycle of CMEs, from their start at the Sun to their propagation through the heliosphere to their geoeffective consequences at Earth. It is essential to understand as well the CME-CME interactions, which can lead to complex ejecta with enhanced geoeffective signatures, often resulting in more intense geomagnetic storms.

2. Data and Method

The prominence eruption was observed at the east solar limb on 2010 June 20 by SDO/AIA. The eruption was observed from two different observation positions and was associated with two CMEs.

For the present study, we used images taken with 1 min cadence in the He II 304 Å and Fe IX 171 Å passbands of the Atmospheric Imaging Assembly [AIA; Lemen at al., 2012] onboard the Solar Dynamics Observatory [SDO; Pesnell et al., 2012]. The AIA consists of seven

Extreme Ultra-Violet (EUV) and three Ultra-Violet (UV) channels, which provide an unprecedented view of the solar corona with an average cadence of ∼12 s. The AIA image field-of-view reaches 1.3 solar radii with a spatial resolution of ∼ 1.5″.

We also analyzed data from the Extreme Ultra-violet Imager (EUVI) onboard the Solar Terrestrial Relations Observatory [STEREO; [29]] Behind (B) spacecraft to investigate the filament eruptions behind the limb. We used data in the He II 304 Å channel with 10 min cadence. Separation angle between STEREO B and Earth at the time of observation was 69.80 degrees.

Images obtained by the Large Angle and Spectrometric Coronagraph (LASCO) onboard the Solar and Heliospheric Observatory [SOHO; Brueckner, 1995] were examined to investigate the associated CME kinematics and related non-radial motion. LASCO has two working coronagraphs, namely, C2 and C3, that observe the Sun in white-light from 2.5 to 30 R⊙. The non-radial offsets of the related CMEs were analyzed by tracking the variations of their position angles (PAs) over time. The PAs are measured counterclockwise from the solar North in degrees. We used the PA of the leading edge of the CME during its propagation in the plane of the sky. For our purposes we used the online CME Catalog at the Coordinated Data Analysis Workshop (CDAW) Data Center [Yashiro at al., 2004], and the "measuring" tool therein. All the data analysis was performed by the solar software (SSWIDL).

3. Filament morphology

The eruption observed by AIA/SDO started on June 19, 2010, at 23:34 UT, at a central position angle (CPA) of 70°, and lasted until 03:00 UT on June 20, 2010, when the prominence material left the instrument's field-of-view (FOV). The prominence was shaped like a loop with two legs anchored in the solar surface. The eruption was of the full type, with no material falling back onto the surface detected. The evolution of the eruption is depicted in Figure 1 within the AIA 171 Å channel, with overplayed contour of the erupting prominence material. The last panel of the figure displays the eruption in a running difference image.

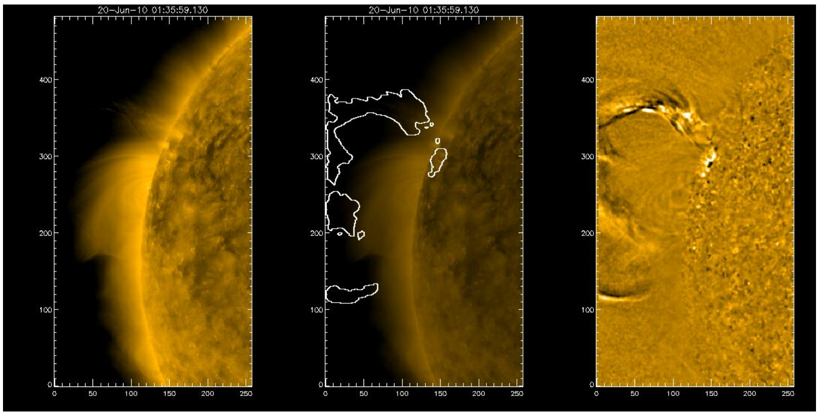

***Figure 1. left:** AIA/SDO 171 Å image, **middle:**the same image with overlay contour of the erupting prominence, and **right:** the differential image (credit: http://eruptivesun.com/).*

In the in EUVI/STEREO–B 304 Å images the eruption was visible on the disk as a filament eruption (Figure 2). Comprising two sections, the filament spans half of the solar hemisphere from the northeast nearly to the equator. The filament began to rise at approximately 01:16 UT, and both components proceeded southward until 03:56 UT.

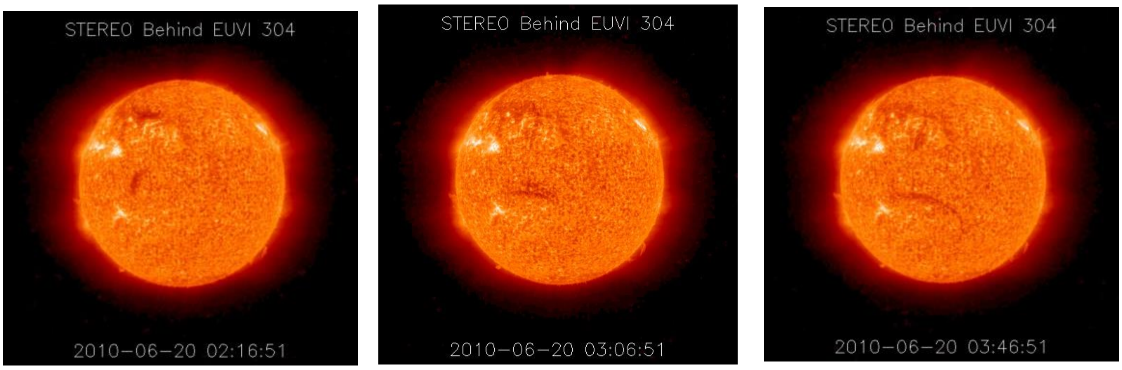

Figure 2. *Evolution of filament eruptions in the 304 Å channel as seen by EUVI/STEREO B.*

4. Eruption kinematic

To examine the event's kinematics, we performed a time-distance analysis. This technique is based on investigating how plasma material moves along an artificial slit. We traced the top of the prominence loop, using AIA/SDO 304 Å data. Figure 3 (left panel) displays the artificial slit that was chosen for the kinematics analysis in the 01:18 UT frame. The corresponding time–distance plot is presented in right panel of Figure 3.

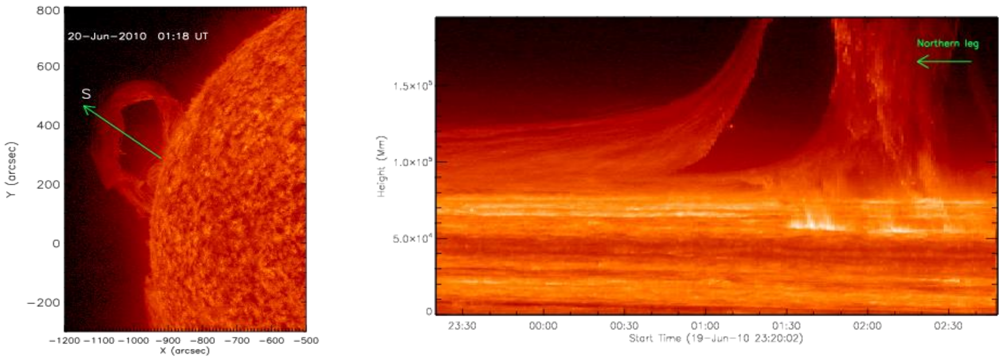

Figure 3. *AIA/SDO 304 Å image, showing the slice position and corresponding time-distance plot.*

From this time–distance plot, we obtained the distance–time data for the leading edge of the erupting prominence. Figure 4A illustrates how the height of the erupting prominence changes over time. The eruption started at 23:34 UT, when the prominence began to slowly rise. It is evident from the time-distance plot that the eruption contains two phases: the slow-rise phase, lasting until 01:30 UT, and the fast rise phase, between 01:30 UT and 03:00 UT, when the prominence material rises rapidly. At around 03:00 UT the top of the prominence loop reached a maximum height at the AIA FOV of 166 Mm above the limb.

The data points of the time-distance plot were fitted with second order polynomial function and the fitted function is plotted as red solid line in Figure 4A. From the first derivative of the polynomial fit of the height-time curve, we defined the speed of the prominence eruption. The velocity changes during the eruption are presented in Figure 4B. During the slow-rise phase the prominence rises with velocity between 0.9 km/s and 9 km/s.

The prominence rises at a speed between 0.9 and 9 km/s during the slow-rise phase, while during the fast-rise phase the velocity increases up to 62 km/s. The prominence loop reached heights of 165 Mm above the solar limb.

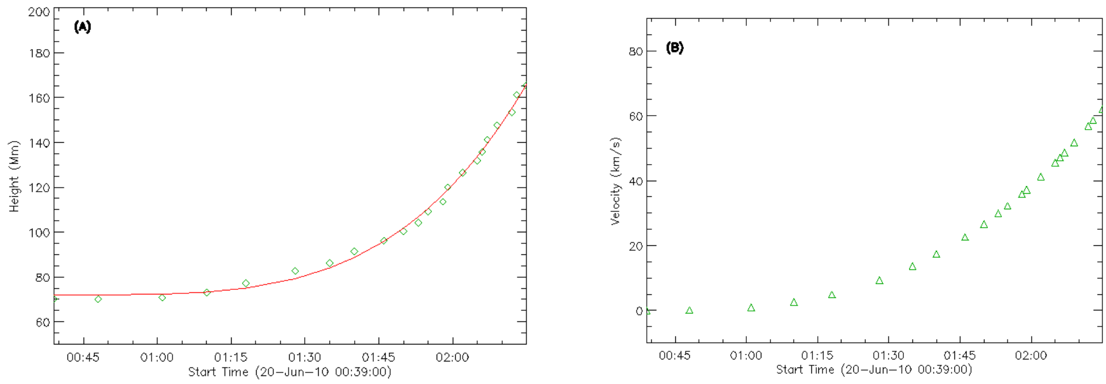

Figure 4. ***(A)*** *Time–distance plot of the prominence eruption. The red solid line is the fitting curve to the data points along the slice.* ***(B)*** *Velocity changes during the eruption.*

5. Associated CMEs evolution

The prominence eruption started at PA of 70° at 23:34 UT the previous day. Two successive CMEs were observed to be associated with the prominence eruption.

Morphology and kimematics

The first CME (CME1) appeared in LASCO/C2 FOV at 23:26 UT, at a CPA of 118°. CME 1 has an angular width of 33° and propagated with a linear speed of 210 km/s and acceleration of about 8 m/s^2. This CME propagated radially in the solar corona.

The second CME (CME 2) first appearance in the LASCO/C2 FOV was at 02:06 UT at a CPA of 108°.

CME2 had an angular width of 93° and propagated at a linear speed of 595 km/s with an acceleration of 6.4 m/s2. The Figure 5 displays the CME2 height-time plot and velocity changes.

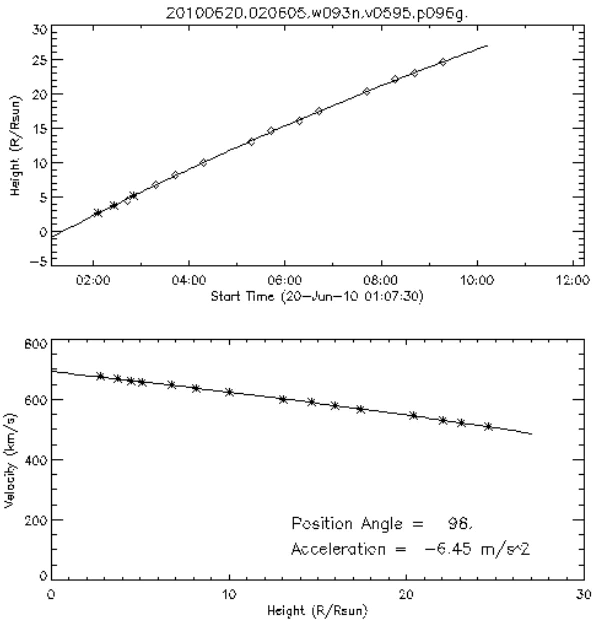

Figure 5. ***(top)*** *Time–distance plot for CME 2.* ***(bottom)*** *Linear velocity changes (image from: https://cdaw.gsfc.nasa.gov/CME_list/index.html).*

CME Deflection

The prominence eruption began at PA of 70°. During the next 4 hr, the CME2 nose and the prominence underwent a significant equatorward deflection to PA of ∼97°. Figure 6 (a) shows the CME2 PA, marked with a red line, at 02:36 UT. At 04:20 UT the CME2 was observed in C3 FOV at PA ∼97° and than continued its propagation without deflection. In Figure 6 (b), the CME2 is shown at 03:26 UT, before it left the LASCO/C2 field of view. The dashed red line points to the CME2 position angle at 03:26 UT, the red line marks the CME2 PA as measured at 02:26 UT, and the double dashed yellow line shows the direction of the initial PA of the PE. Thus the PA offset between the initial PE location and the CME2 nose was 27° towards the equator.

After 08:42 UT the two CMEs in LASCO/C3 look like one twisted common structure at PA ~ 123°. In LASCO/C3 running difference images, this event could be traced up to 26 solar radii and propagated in the solar corona without appearing to deviate from the radial direction (see Figure 6, c).

The time variations of the CME2 core and nose are shown in Figure 7(a). We also examined the variation of the PA with heliocentric distance and the result is presented in Figure 7(b). The non-radial motion stopped at about 9 $R_\odot$.

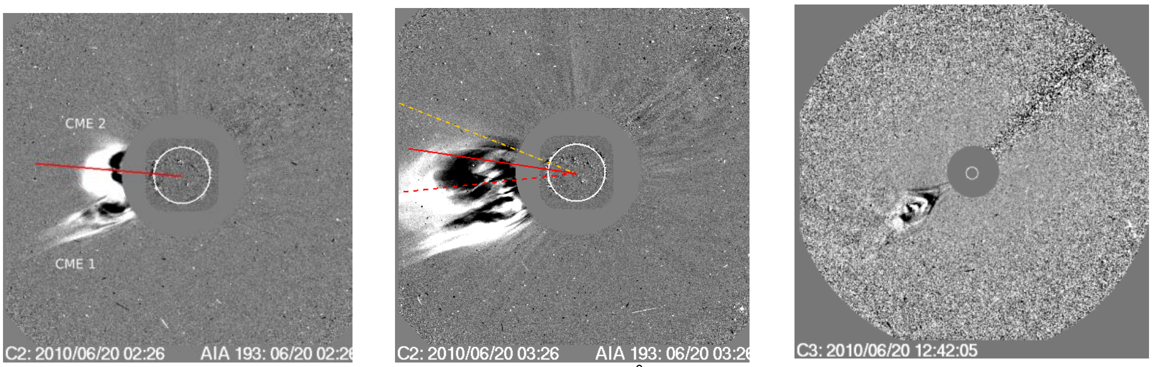

Figure 6. *(a) SOHO/LASCO/C2 and AIA/SDO 193 Å composite image at 02:26 UT. The red line denotes the CME2 PA (b). SOHO/LASCO/C2 and AIA/SDO 193 Å composite image at 03:26 UT. The CME2 PA for 02:26 UT and 03:26 UT and PE PA are shown by red, dashed red and double dashed yellow lines, respectively. (c) Running difference images from LASCO/C3 coronagraph at 12:42 UT.*

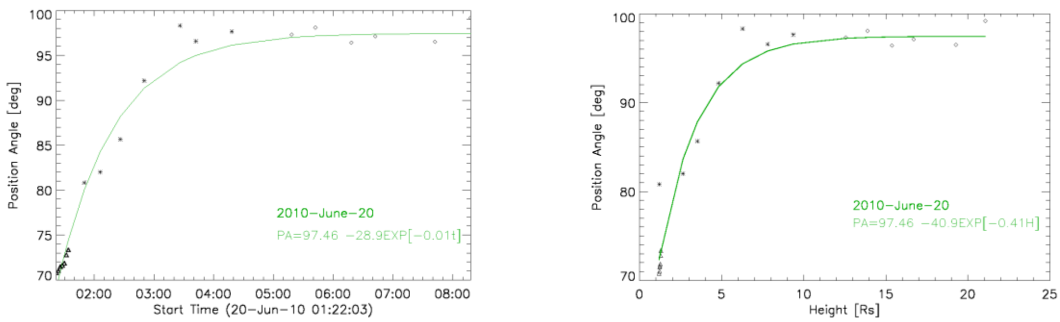

Figure 7. *(a) Variation of the position angle of CME core and nose as a function of time. Triangles, stars, and diamonds represent measurements, respectively in AIA FOV, from C2, and C3 coronagraph of SOHO/LASCO. (b) CME Position angle (PA) at various heliocentric distances. The solid line is the fit to the data points, showing that the non-radial motion stopped at about 9 $R_\odot$.*

6. Results

We examine the morphology and kinematics of the June 20, 2010. The prominence eruption that took place in the east solar limb and was observed by AIA/SDO and STEREO B observatory. The eruption in the AIA FOV was followed by two successive CMEs, which we named CME 1 and CME 2.

The results from the study can be summarized as follows:

- ✓ The eruption observed by AIA/SDO started at CPA of 70° at 23:34 UT on the previous day and lasted until 03:00 UT on June 20, 2010. During this time period the images obtained by the EUVI/STEREO–B show a huge disk filament, consisting of two distinct parts. The eruption of the two components of that filament could be interpreted as the cause of the two observed CMEs.
- ✓ The kinematics characteristics of the prominence eruption, as observed by AIA/SDO, reveal two eruptive phases. During the slow-rise phase, between 23:34 UT and 01:30 UT, the prominence slow rises with velocity between 0.9 km/s and 9 km/s. This phase was followed by a fast-rise phase with velocity of 62 km/s. Before leaving the AIA FOV, the prominence loop reached a height of 165 Mm above the solar limb.
- ✓ The eruption was associated with two CMEs, namely, CME1 and CME 2. CME1 appeared at CPA of 118° and propagated radially in the solar corona with a linear speed of 210 km/s and acceleration of about 8 m/s^2.
- ✓ CME 2 started at CPA of 108°. It demonstrated substantial non-radial motions while propagating at a linear speed of 595 km/s with an acceleration of 6.4 m/s^2. The latitudinal offset between the initial PE location and the CME2 nose was 27° towards the equator. Such deflection can be attributed to the influence of a polar coronal hole (CH).
- ✓ The two CMEs seemed to be one twisted common structure around 08:42 UT, most likely due to their interaction. This structure spread radially in the solar corona and could be traced up to 26 $R_\odot$.

References

Brueckner, G.E. (1995). The Large Angle Spectroscopic Coronagraph (LASCO), *Solar Physics*, Vol. 162, pp. 357–402, DOI: 10.1007/BF00733434.

Forbes, T.G. (2000). A review on the genesis of coronal mass ejections, *Journal of Geophysical Research: Space Physics*, Vol. 105, No. A10, pp. 23153–23166, DOI: 10.1029/2000JA000005.

Gopalswamy, N., Thompson, B.J. (2000). Early life of coronal mass ejections, *Journal of Atmospheric and Solar–Terrestrial Physics*, Vol. 62, pp. 1457–1469, DOI: 10.1016/S1364-6826(00)00079-1.

Kaiser, M.L., Kucera, T.A., Davila, J.M., et al. (2008). The STEREO mission: An introduction, *Space Science Reviews*, Vol. 136, pp. 5–16, DOI: 10.1007/s11214-007-9277-0.

Koleva, K., Gopalswamy, N., Devi, P., Yashiro, S., Michalek, G. (2024). Spatial relationship between CMEs and prominence eruptions during solar cycles 24 and 25, *Astrophysical Journal*, Vol. 966, 22, DOI: 10.3847/1538-4357/ad2df3.

Lemen, J.R., Title, A.M., Akin, D.J., et al. (2012). The Atmospheric Imaging Assembly (AIA) on the Solar Dynamics Observatory (SDO), *Solar Physics*, Vol. 275, pp. 17–40, DOI: 10.1007/s11207-011-9776-8.

Mackay, D.H., Karpen, J.T., Ballester, J.L., Schmieder, B., Aulanier, G. (2010). Physics of solar prominences: II — Magnetic structure and dynamics, *Space Science Reviews*, Vol. 151, pp. 333–399, DOI: 10.1007/s11214-010-9628-0.

Parenti, S. (2014). Solar prominences: Observations, *Living Reviews in Solar Physics*, Vol. 11, pp. 1–89, DOI: 10.12942/lrsp-2014-1.

Pesnell, W.D., Thompson, B.J., Chamberlin, P.C. (2012). The Solar Dynamics Observatory (SDO), *Solar Physics*, Vol. 275, pp. 3–15, DOI: 10.1007/s11207-011-9841-3.

Priest, E.R., Forbes, T.G. (2002). The magnetic nature of solar flares, *Astronomy and Astrophysics Review*, Vol. 10, No. 4, pp. 313–377, DOI: 10.1007/s001590100013.

Sterling, A., Harra, L., Moore, R. (2007). New evidence for the role of emerging flux in a solar filament's slow rise preceding its CME-producing fast eruption, *Astrophysical Journal*, Vol. 669, pp. 1359–1371, DOI: 10.1086/520829.

Tandberg-Hanssen, E. (1995). *The Nature of Solar Prominences*, *Astrophysics and Space Science Library*, Vol. 199, Kluwer Academic Publishers, Dordrecht, The Netherlands, DOI: 10.1007/978-94-017-3396-0.

Yashiro, S., Gopalswamy, N., Michalek, G., et al. (2004). A catalog of white light coronal mass ejections observed by the SOHO spacecraft, *Journal of Geophysical Research: Space Physics*, Vol. 109, A07105, DOI: 10.1029/2003JA010282.